Characterization of a Synthetic Anionic Vector for Oligonucleotide Delivery Using *in Vivo* Whole Body Dynamic Imaging

Bertrand Tavitian,[1,6] Stéphane Marzabal,[1] Valérie Boutet,[3] Bertrand Kühnast,[1,2] Salvatore Terrazzino,[1] Marinette Moynier,[4] Frédéric Dollé,[2] Jean Robert Deverre,[3] and Alain R. Thierry[4,5]

Received July 9, 2001; accepted January 4, 2002

Purpose. To compare the pharmacokinetics and bioavailability of an oligonucleotide delivered in a free form or using cationic or anionic synthetic carrier systems.

Methods. Whole body dynamic quantitative imaging and metabolism of a HIV antisense oligonucleotide intravenously administered either free or incorporated into synthetic carriers were compared in baboons, using non invasive positron emission tomography and an enzyme-based competitive hybridization assay, respectively.

Results. In its free form, the oligonucleotide showed high liver and kidney concentration, rapid plasmatic degradation and elimination from the body. Use of a cationic vector slightly protected the oligonucleotide against degradation and enhanced uptake by the reticuloendothelial system. In contrast, the anionic vector dramatically enhanced the uptake in several organs, including the lungs, spleen and brain, with a prolonged accumulation of radioactivity in the brain. Using this vector, intact oligonucleotide was detected in plasma for up to two hours after injection, and the $T_{1/2}\beta$ and distribution volume increased by 4- and 7-fold, respectively. No evidence of toxicity was found after a single dose administration.

Conclusions. The anionic vector improves significantly the bioavailability and the pharmacokinetics of the oligonucleotide, and is a promising delivery system for *in vivo* administration of therapeutic nucleic acids.

KEY WORDS: antisense oligonucleotide; *in vivo* delivery; Neutraplex; positron emission tomography (PET); pharmacokinetics.

INTRODUCTION

Oligonucleotides are a class of compounds with wide biologic activities and the subject of increased scrutiny in the field of molecular medicine. The key to their successful pharmaceutical applications as antisense, aptamers, ribozymes, etc is to achieve efficient *in vivo* delivery. Systematically administered oligonucleotides must escape plasmatic and tissular nucleases and cross various biological membranes to reach their cellular target. Hence, technological tricks are necessary to circumvent the efficient mechanisms by which living organisms protect themselves from an invasion by exogenously administered nucleic acids. One widely explored possibility consists in modifications of the natural oligonucleotides' backbone that enhance their stability. However, chemical modifications may decrease sequence specificity and/or activity of oligonucleotides, and have little or no effect or may even be deleterious for membrane passage (1).

Another line of research is to incorporate oligonucleotides into synthetic vectors acting as Trojan's horses (2), that would at the same time protect them against nucleasic attack and direct them inside cells. Synthetic vectors are mantailored on the basis of their known physico-chemical properties and can be repeatedly administered. Complexes of DNA with cationic lipids (lipoplex) (3) result in the respective condensation of both entities by way of electrostatic interactions. One of the crucial impediments for successful systemic oligonucleotides or DNA transfer with lipoplex exhibiting a positive global charge seems to be their inactivation due to non-specific binding with anionic serum proteins. We have designed a unique formulation process allowing preparation of stable and homogenous lipoplex particles, called Neutraplex™, exhibiting a negative global charge.

However, efforts undertaken to develop synthetic vectors for nucleic acids delivery remain gratuitous as long as their efficiency in improving the bioavailability and resistance to degradation of the active ingredient cannot be demonstrated *in vivo*. Although encouraging results were obtained after injection of vectorized DNA, they all showed a lack of power in resolution and analysis due to the procedures used (4,5).

Positron emission tomography (PET) is a highly sensitive, non-invasive medical imaging technique, which is remarkably suited for *in vivo* evaluation of drug pharmacokinetics or activity (6,7). We have recently applied this technology to whole body quantitative imaging of nucleic acids (8). In addition, we have developed an ultra-sensitive competitive hybridization assay to determine the stability of nucleic acids in plasma and tissue samples (9).

In this study, we combined both methods to compare the whole body biodistribution, imaged quantitatively with PET, and the stability, assessed by competitive hybridization, of a phosphodiester octodecanucleotide delivered intravenously to non-human primates, either in a free form, with a classical cationic lipid complex, or with a new anionic synthetic carrier. The combination of the two techniques described here demonstrates that a carefully tailored anionic vector can dramatically improve *in vivo* delivery of an oligonucleotide by increasing its plasmatic half-life and biodistribution.

METHODS

Oligonucleotide

Dis-2 is a phosphodiester octodecanucleotide (5′CTCTTGCCGTGCGCGCTT3′) obtained from Eurogentec (Seraing, Belgium). Dis-2 is the shorter version of Dis, an antisense octoeikosinucleotide directed to a highly conserved sequence of the dimerization site of the LTR region of HIV (10). Com-

[1] INSERM M 0103, CEA – SHFJ, 4 place du général Leclerc, F-91401 Orsay cedex - France.
[2] Groupe de Radiochimie, Service Hospitalier Frédéric Joliot, CEA, Orsay, France.
[3] Service de Pharmacologie et d'Immunologie, CEA, Gif-sur-Yvette, France.
[4] Biovector Therapeutics, Labège, France.
[5] Med in Cell Project, Laboratoire des Défenses Antivirales et Antitumorales, UMR 5124, 1919 route de Mende, 34293 Montpellier Cedex 5, France.
[6] To whom correspondence should be addressed: (e-mail: tavitian@shfj.cea.fr)

0724-8741/02/0400-0367/0 © 2002 Plenum Publishing Corporation

puter search in databases showed no relevant complementary sequence other than Homo sapiens cadherin V mRNA and *Escherichia coli* K-12, which have 16 and 15 nucleotides out of 18, respectively, matching with Dis-2.

Radiosynthesis

The labeling and quality control of oligonucleotides were as previously described (11). Typical radiosynthesis yields were 5.18×10^8 Bq (14 mCi) of [^{18}F]-Dis-2 at the end of synthesis with a specific radioactivity of 1.55×10^{11} Bq/μmole (4.2 Ci/μmole) calculated from end of bombardment.

Formulation

Cationic Lipoplex

Formulation of Dis-2 with cationic lipoplexes (DD) is derived from the DLS formulation as previously described (12). Small Unilamellar Vesicles (SUV) were formed by mixing 1.5 mg dioctadecylamidoglycylspermidine (DOGS, Biosepra) with 1 mg dioleoylphosphatidylethanolamine (DOPE, Sigma) in ethanol and subsequently by adding pure water (final lipid concentration 6.25 mg/mL). Just before injecting the baboon, formation of DD lipoplex was carried out by mixing SUV suspension with two volumes of NaCl 20 mM. The oligonucleotide solution was then mixed with the diluted SUV (final concentrations, oligonucleotide 0.12 mg/mL, lipid 1.25 mg/mL). The zeta potential of the two DD formulations administered *in vivo* were +4.5 and +37.3 respectively, as measured with a Zetasizer 3000 (Malvern Instruments, Paris). Their sizes were 71.5 nm and 87.7 nm with a polydispersity of 0.277 and 0.244, respectively.

Anionic Lipoplex

Anionic lipoplex Neutraplex™ (NX1) formulation of Dis-2 was performed as previously described (13). SUV were formed by mixing 1.8 mg of GLB43 cationic lipid (14) provided by Dr Clement of the University of Brest, 0.5 mg cholesterol (Sigma) and 0.5 mg natural cardiolipin (Sigma), in ethanol and subsequently by adding pure water (lipid concentration 2.33 mg/mL). Just before injection, SUV were diluted in water (final lipid concentration 2.0 mg /mL,) and formation of the NX1 lipoplex was carried out by adding the diluted SUV to an equal volume of oligonucleotide solution followed by pure water (final concentrations, oligonucleotide 0.12 mg/mL, lipid 0.6 mg /mL). The level of Dis-2 incorporation in NX1 was 94 ± 8%. The zeta potential of the two NX1 formulations administered *in vivo* were −35.6 and −34.0 respectively. Their size was 162.7 nm and 171.5 nm with a polydispersity of 0.079 and 0.112 respectively.

The oligonucleotide solution (final concentration, 1 mg/mL) used for the lipoplex preparations was a mixture of [^{18}F]-Dis-2 and unlabeled Dis-2 in sterile water, in which the radiolabeled oligonucleotide represented less than 1% of the total amount of Dis-2. All preparations were calibrated so that the animals received a dose of 100.9 ± 0.4 μg per kg of body weight of Dis-2 in a volume of 2–3 mL.

Plasma Analysis

Labeled Oligonucleotide Analysis

Arterial blood samples were drawn during the PET acquisition in tubes containing 2.5 mM EDTA at designated times after injection. Blood was centrifuged 10 min at 3000 rpm at 4 °C (Jouan C3.12, Paris) and weighed aliquots of blood and plasma were counted on a CG 4000 gamma counter (Intertechnique, France). Radioactivity concentration was expressed as fraction of injected dose.

Sample Preparation

Oligonucleotides and metabolites were extracted from plasma by adding one volume of phenol-chloroform (mixture in equal proportions) and four volumes of Tris-EDTA (TE, pH 8). The mixture was centrifuged at 13,000 rpm for 10 min. Pellet was extracted with an additional 200 μl of TE. Supernatants were collected, vacuum dried and dissolved in a known volume of water before injection on the analytical RP-HPLC.

High-Performance Liquid Chromatography

Analytical RP-HPLC was performed with a 600 Controller Pump (Waters, St Quentin en Yvelines, France) and a UV detector series 1100 (Hewlett Packard, Les Ulis, France). Radioactivity was counted on line with a Flow Scintillation Analyzer Detector (Packard, Rungis, France). The column was a μBondapak C_{18} 3.9 × 300 mm (Waters, St·Quentin en Yvelines, France) and gradient elution was done with a mixture of TEAA (A) and Acetonitrile (B). The gradient (A/B) was linear 3 min from 95/5 to 90/10, linear 17 min from 90/10 to 80/20. Finally the column was washed out with 80% Acetonitrile before reequilibration.

Unlabeled and Labeled Oligonucleotide Analysis by Heterogeneous Competitive Enzyme Hybridization Assay

Oligonucleotides were synthesized by Eurogentec (Seraing, Belgium). Competitive hybridization assay was performed as previously described (9). Data were analyzed using Immunofit EIA/RIA (Beckman, CA) software and by applying the four parameter logistic transformation. The method was validated as previously described (8) in baboon plasma samples and with the sequences included in Table I. Validation parameters were assessed with three quality control samples of baboon plasma. Acceptable intra- and inter-assay were obtained in the range of calibration 262–1046 fmol/mL. The limit of quantification was 256 fmol/mL. The percentage of cross reactivity obtained with Dis-2-related oligomer deleted at the 3′ and 5′ end (N-1 to N-3), were lower than 30% (Table I). No interference with any compounds of either formulation was observed. The percentage of cross-reactivity between unlabeled and [^{18}F]-labeled- Dis-2 was 100%, indicating that the labeling has no impact on the hybridization assay of Dis-2.

Imaging Studies

Animal Handling and Treatment

All experiments were conducted in agreement with French and European animal experimentation regulation. Two noninfected (SIV and HIV-free) male *Papio papio* baboons weighing 7.5 kg and 8.3 kg were used for the crossover experiments. A one-week washout period was observed between each experiment. Ninety minutes before the PET ex-

Table I. Sequence of the Oligonucleotides Used and Percentage of Cross-Reactivity Coefficients Measured in Monkey Plasma

Name	Sequence	Cross reactivity (%)
Dis-2 oligonucleotide	5′-CTCTTGCCGTGCGCGCTT	100
Tracer oligonucleotide	5′-biotin CTCTTGCCGTGCGCGCTT	
Capture oligonucleotide	5′ phosphate	
fixed to the microwells	AAAAAAAGTGCAATACACCTGAAGCGCGCAC	
complementary to Dis-2	GGCAAGAGAGTGCAATACACCTG	
3′ deletion of oligonucleotide Dis-2		
3′ N-1	5′-CTCTTGCCGTGCGCGCT	25
3′ N-2	5′-CTCTTGCCGTGCGCGC	20
3′ N-3	5′-CTCTTGCCGTGCGCG	5
5′ deletion of oligonucleotide Dis-2		
5′ N-1	5′-TCTTGCCGTGCGCGCTT	30
5′ N-2	5′-CTTGCCGTGCGCGCTT	21
5′ N-3	5′-TTGCCGTGCGCGCTT	7

amination, baboons were pre-anaesthetized with ketamine 10 mg/kg IM, then intubated and ventilated with a mixture of O_2 and N_2O in a one-third / two-third proportion with isoflurane anesthesia (1%) under constant respiratory and cardiac monitoring. Venous (for injection) and arterial (for blood sampling) catheters were introduced. Major biological parameters (blood formula, sedimentation velocity, hepatic, pancreatic and cardiac enzymes) were controlled routinely in the animals and showed no variation from normal parameters.

Positron Emission Tomography Data Analysis

PET scans were acquired with the ECAT EXACT HR+ camera (63 slices, spatial resolution with a Hanning 0.5 reconstruction filter: 4.5 mm × 4.5 mm × 2.25 mm at full-width half maximum) in 3D acquisition mode. Correction for 511 keV gamma-ray attenuation by tissues was performed based on ^{68}Ge-^{68}Ga transmission scans. A sequence of 20 scans covering 120 min (20 × 6 min) were acquired after the injection. The injected dose ranged from 18.5 to 92.5 MBq (0.5 to 2.5 mCi) with a specific radioactivity of 28.3 ± 28.7 GBq/μmole (764 ± 777 mCi/μmole) and always represented a total Dis-2 load of 100.9 ± 0.4 μg/kg, whether free or vector-associated. The kinetics of radioactivity concentrations in organs was obtained by tracing regions of interest using CAPP software (CTI, Knoxville, USA). To allow for comparison the radioactivity concentrations were normalized for the injected dose, and graphical normalization software was developed in IDL language running on UNIX stations. Images in 32-bit format were corrected for the radioactivity decay and for the injected dose, and depicted on a standard color scale expanded between the minimum and maximum of the whole volume of acquisition.

Pharmacokinetics Analysis

Pharmacokinetics analysis was performed using Kinetica software (SIMED SA, Créteil, France). Both a one- and a two-compartment model were used to estimate the half-life ($T_{1/2}$), the area under plasma concentration-time curve (AUC), the distribution volume (Vss) and the clearance (Cl) of Dis-2. Since both models gave similar results, the results from the two-compartment model are presented in accordance with previous pharmacokinetics studies of oligonucleotides (15). AUC_{120} was calculated by the trapezoidal method.

RESULTS

Pharmacokinetics and Metabolism in Plasma

The plasma pharmacokinetics of labeled Dis-2 and unlabeled intact Dis-2, assessed by the competitive hybridization assay, are reported in Fig. 1. Plasma profiles of Dis-2 after IV administration in its free or cationic vector DD delivered-forms were similar (Fig. 1A and 1B). Free or DD-formulated Dis-2 (DD/Dis-2) was rapidly distributed and metabolized: $T_{1/2}\beta$ was 10.6 ± 2.7 min for free Dis-2 and 5.7 ± 0.8 min for DD/Dis-2 (Table II). Intact Dis-2 was undetectable after 30 min. Plasma clearances were 176 ± 13 mL/min and 205 ± 30 mL/min for free Dis-2 and DD/Dis-2, respectively, and the distribution volumes (Vss) were 742 ± 497 mL and 556 ± 91 mL for free Dis-2 and DD/Dis-2, respectively.

The plasma kinetics of NX1-associated Dis-2 (NX1/Dis-2) was similar at early times after injection but significantly differed afterwards (Fig. 1C), and Dis-2 was still present in plasma 2 h after injection. Analysis of pharmacokinetics parameters confirmed this observation (Table II) though AUC and clearance were not affected by NX1 vectorization. $T_{1/2}\ \beta$ (44 ± 2 min) increased by a factor of 4 and 8, and Vss (5472 ± 678 mL) increased by a factor of 7 and 10, when compared to free Dis-2 and DD/Dis-2 values, respectively.

Radio-HPLC analysis showed that, for all formulations, the majority of radioactivity recovered from plasma 5 min after [^{18}F]Dis-2 administration was associated with intact Dis-2, and little (<5%) degradation was seen at this early time. Thirty minutes after injection of free or DD/Dis-2, no intact Dis-2 could be detected in the plasma that contained only radioactive metabolites. In contrast, NX1 vectorization led to a recovery of 5–10% of intact Dis-2 in plasma up to 60 min post-injection.

Whole Body *in Vivo* Imaging

Representative PET images of the distribution of radioactivity concentrations after [^{18}F]-Dis-2 administration are shown in Fig. 2 and the corresponding pharmacokinetics are

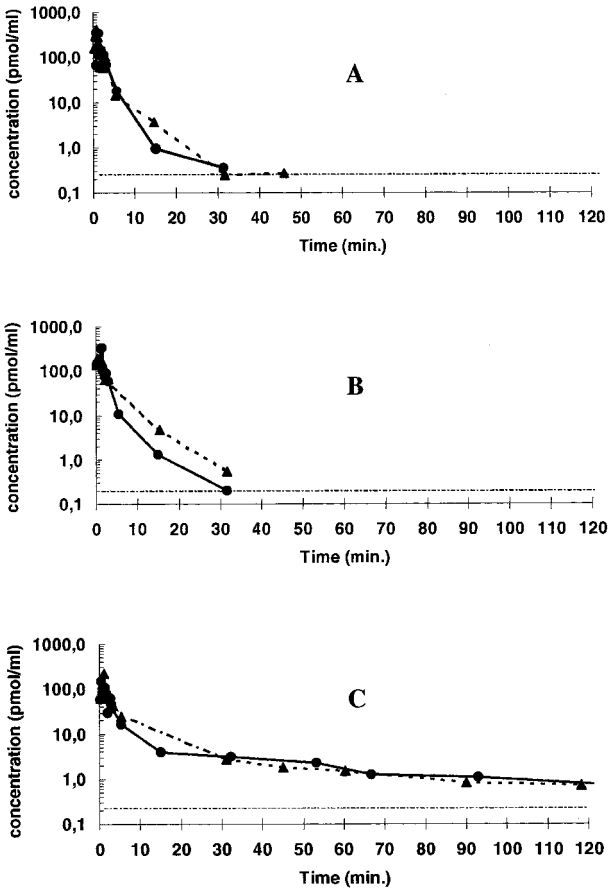

Fig. 1. Plasma kinetics after IV bolus of Dis-2 free (A) or delivered with DD (B) and NX1 system (C). Dashed line: limit of quantification of the competitive hybridization assay. Circles, baboon A, triangles, baboon B.

shown in Fig. 3. With free Dis-2, radioactivity was highly concentrated in the kidneys and in the liver already at 5 min after injection. Accumulation in the bladder began within 10 to 40 min and coincided with a renal purge of the radioactivity. The distribution of radioactivity was not significantly modified by DD vectorization, except in the organs of the reticulo-endothelial system, the liver and spleen. In these two organs, DD induced an increase of the radioactivity concentration (20% and 190% increase of the AUC_{120} for liver and spleen, respectively), and in the liver, the peak of radioactivity appeared earlier with DD/Dis-2 (10 min) than with free Dis-2 (30 min).

In contrast, NX1 delivery induced major changes in the distribution of radioactivity in all organs, with the exception of the heart, where pharmacokinetics remained unchanged as compared with free Dis-2 or DD/Dis-2. It should be noted that there was a major contribution of blood to the heart radioactivity, as shown by the superimposition of the blood and heart radioactivity–over-time curves. In the lungs, NX1 induced an increase of the maximal concentration at initial peak and a slower decrease of the signal after the peak, leading to a 3- to 4-fold increase of the AUC_{120} when compared with free Dis-2. The same increase was observed in the spleen (AUC_{120}, 6–7-fold increase). Despite an increase of the initial peak value, the radioactivity in the liver rapidly returned to the level observed with free Dis-2, thus there was only a limited (50%) increase in the AUC. No effect of NX1 vectorization was observed on the renal uptake or bladder accumulation during the 2 h following injection. The most radical change induced by NX1 was observed in the brain, in which both an increase of the radioactivity uptake and a modification of the pharmacokinetics were prominent. At early times, brain radioactivity concentrations were identical with free, DD or NX1 vectorized Dis-2, and showed a peak between 5 and 10 minutes followed by a decrease. Thereafter, in contrast to free or DD/Dis2, NX1/Dis-2 induced a second phase of cerebral radioactivity accumulation starting at 20 min post-injection and persisting until the end of the PET acquisition. This observation was highly reproducible between the two animals.

Images normalized for the injected dose allow direct comparison of the radioactivity concentrations in the organs of interest (Fig. 4). The higher uptake of radioactivity in the spleen and lungs with NX1/Dis-2 is clearly depicted, as well as the dramatic change in the cerebral distribution of radioactivity induced by NX1. In contrast to free Dis-2 in which radioactivity was localized around the brain area and did not seem to penetrate the tissue, with NX1/Dis-2 radioactivity was localized inside the cerebral area. This result prompted us to repeat the same experiment with a longer and more precise acquisition centered on the cephalic area (Fig. 5). Results were similar, with a steady intracerebral accumulation of radioactivity starting around 25 min and continuing thereafter. Due to the 110 min half-life of Fluorine-18, it was not possible to pursue PET acquisition longer than 360 min, but a plateau of cerebral uptake was not reached even at this time.

Finally, toxic effect is of concern when injecting large complexes, especially by intravenous route. It has been reported for instance that lipoplex activates human complement *in vitro* (16) and leads *in vivo* to depletion of plasmatic complement in mice. We found no evidence of toxicity, neither on clinical examination of the animals, nor on blood tests exploring adverse hematological, hepatological, renal and muscular effects, with the single dose used in this study (lipid 50 μg/kg and oligonucleotide 100 μg/kg).

DISCUSSION

Although the antisense approach is conceptually simple and elegant, its practical application to *in vivo* situations resembles the difficult navigation between the rocks of Charybdis and Scilla. Too often, chemical modifications that allow the antisense to escape nuclease destruction, such as the phosphorothioate, lead to biologic effects solely or partly non-specific in nature (1). Combinations of different backbone chemistries in the same oligonucleotide are now being explored in the so-called "mixed backbone oligonucleotides" or "gapmers", with the hope that these compounds will keep the benefits and avoid the drawbacks of each chemical modification. The use of vectors that coat the antisense is another approach, which offers the opportunity to enhance delivery through increased membrane passage and to be applicable to any sequence without tedious optimizations. This approach was explored here with the oligonucleotide Dis-2, derived from Dis, an HIV-1 antisense octoeikosinucleotide that showed a potent antiviral activity and could block HIV-1 replication in acutely and chronically infected cells for up to 21

Table II. Plasmatic Pharmacokinetics Parameters of Dis-2 after IV Bolus of Free or Encapsulated Dis-2 in DD and NX1 in Baboons. Two Compartmental Analysis

	Unmodified parameters								
Treatment	Dis-2		DD-Dis-2		NX1/Dis-2				
Baboon	1	2	1	2	1	2	Mean	SD	CV%
Dose (nmol)	146	136	146	136	146	136	141	5	4
AUC (nmol/mL.min)	.88	.74	.79	.60	.68	.70	.73	.1	13
Clearance (mL/min)	170	190	18	230	210	200	200	22	11
	Modified parameters								
Treatment	Dis-2		DD/Dis-2						
Baboon	1	2	1	2	Mean	SD			
$T_{1/2}$ β (min)	12.5	8.7	5.1	6.3	8.7	3.7			
Vss (L)	0.4	1.1	.6	.5	.7	.4			
Treatment	NX1/Dis-2								
Baboon	1	2	Mean	SD					
$T_{1/2}$ β (min)	42.4	45.5	44.0	2.2					
Vss (L)	6.0	5.0	5.5	.7					

days (10). Dis-2 is an octodecanucleotide and a candidate antisense drug whose size falls in the range employed in the oligonucleotide research field. As a phosphodiester, Dis-2 is highly biodegradable and thus well suited for exploring the *in vivo* fate of an oligonucleotide following delivery. The mechanisms of activity of Dis and Dis-2 are under investigation to evaluate the potential of these antisense oligonucleotides. The fact that the effect of Dis was found sequence specific only in a short term assay using MOLT-3 acutely infected cells, among other cell models tested, and when delivered with the DLS system, prompted us to examine the capacity of synthetic vectors to protect and deliver Dis-2 *in vivo*.

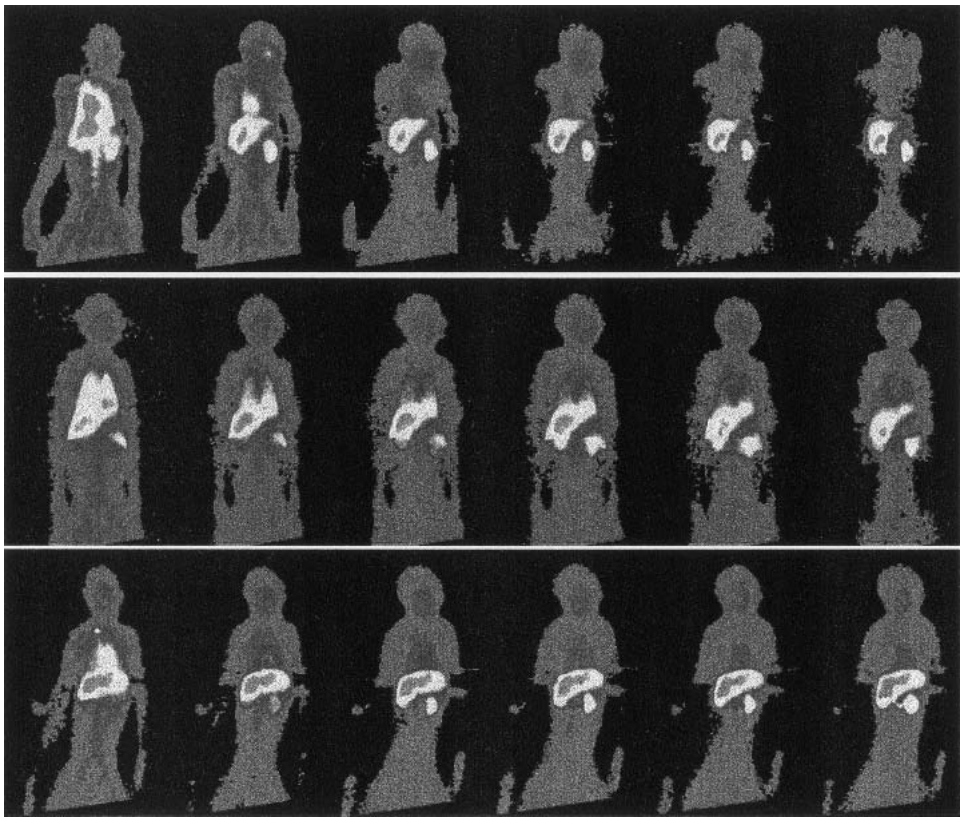

Fig. 2. Whole body PET images of radioactivity distribution after injection of free (upper panel) or vector-associated Dis-2 (NX1, middle panel; DD lower panel). Median time intervals after injection are, from left to right, 3, 10, 16, 23, 29, 35 min. Gray scale is from black (zero radioactivity) to white (maximal radioactivity concentration).

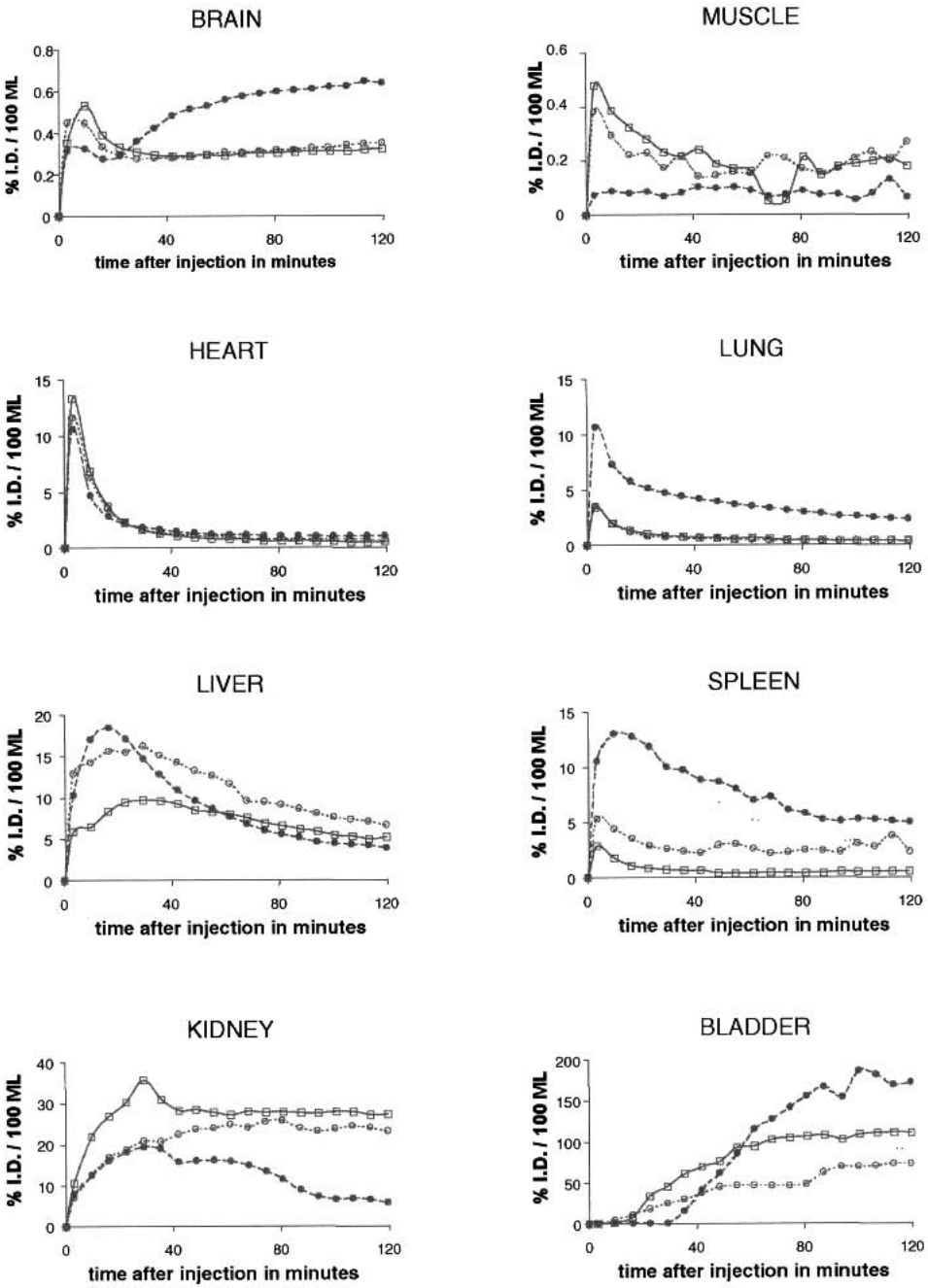

Fig. 3. Pharmacokinetics in heart, lung, liver, spleen and brain. Concentrations of radioactivity in the organs expressed as the percentage of the injected dose per volume of tissue. (□): free Dis-2; (○): DD/DIS-2; (●): NX1/Dis-2.

Despite the numerous efforts undertaken to develop efficient synthetic vectors, there is little evidence of satisfactory *in vivo* nucleic acids delivery after intravenous administration (5,17). Liposomes and polymeric nanoparticles have either low encapsulation efficiency or low drug/lipid ratios, or both (18,19,20). Use of cationic constituents to closely associate and condense nucleic acids within particles considerably reduces those limiting factors. However, most of these systems termed as lipoplex (3) form heterogeneously sized particles of positive global net charge. This property may lead to potential toxicity (21), serum protein binding (22), complement activation (16) and low circulation time following systemic administration (21, 23). Neutraplex™ is a new anionic vector, showing high particle size homogeneity, high stability in biologic media and *in vitro* transfection activity equivalent to commercially available cationic systems. Physical and microscopic analysis demonstrated that Neutraplex™ forms spherical multilamellar particles with a distinct concentric ring-like pattern (13). The ultrastructure and particle size distribution of Neutraplex™ appear similar upon incorporation of nucleic acids of different types and sizes such as plasmid DNA and oligonucleotides (13).

To evaluate the efficiency of this type of anionic vector *in vivo*, Neutraplex™ (NX-1, global net charge of 0.75) was

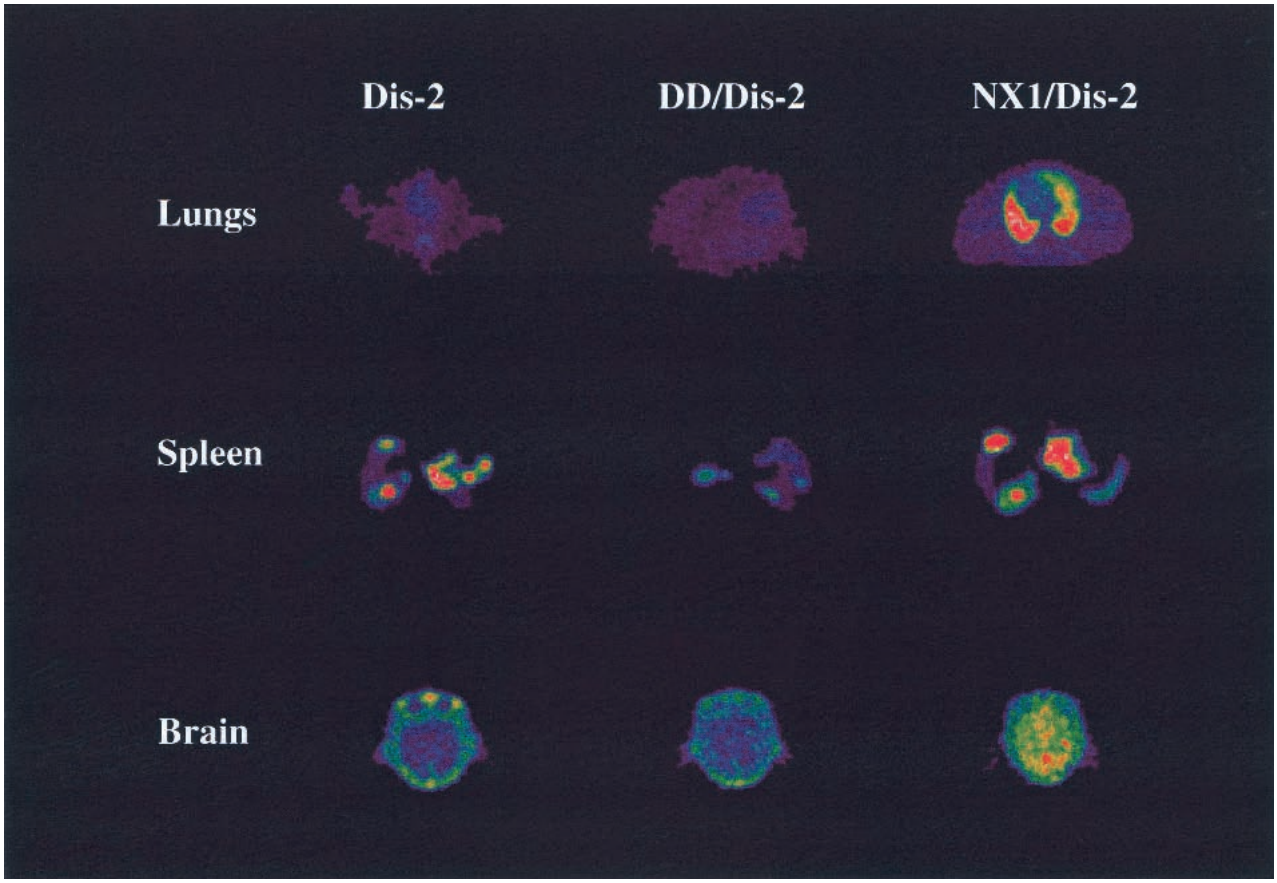

Fig. 4. Normalized images of PET acquisition for the lungs, spleen and brain in baboon A after different treatments. These images represent the sum of the time frames acquired between 60 and 120 min after IV injection of radiolabeled Dis-2, free or vectorized, in one transaxial tomographic slice (2.425 mm thickness). Images taken at the same anatomic level are corrected for the radioactivity decay, normalized for the injected dose, and depicted with the same color scale (black = zero to red = maximum) to allow a direct comparison of the different formulations. Images are representative of the two baboons.

compared with a conventional cationic lipoplex which exhibited similar stability and homogenous particle size but a global net charge (3) of 5. Complexes of Dis-2 and both cationic and anionic vectors were obtained under tight control of formulation parameters. The cationic lipoplex (DD) was derived from the DLS preparation (12, 24, 25) using the lipids DOGS and DOPE, but exhibited higher global net charge (5 vs. 2.5). The anionic vector Neutraplex™ (NX1) was constituted by three molecules of different charge: DOPE (neutral), cardiolipin (anionic) and GLB43, a monocationic phosphonolipid developed by Clément and Ferec (14).

This work focused on the *in vivo* characterization of ODN delivery using a novel synthetic carrier system, Neutraplex, and aimed at defining its pharmacokinetic potential to deliver an oligonucleotide, rather than at achieving a specifically targeted pharmacokinetics. Results suggest that NX1 (i) decreased ODN plasma clearance; (ii) facilitated distribution in organs such as lungs, brain and spleen over free ODN and (iii) targeted the brain. In contrast to most of the other lipoplex formulations so far developed, the high particle size homogeneity and stability of both preparations made possible IV injection without endangering the animals.

To our knowledge there is no published study comparing the pharmacokinetics of phosphodiester oligonucleotide administrated in free form and with a synthetic vector. There is as well no report on the biodistribution in primates of oligonucleotides delivered intravenously with a carrier. Positron emission tomography is increasingly used in drug design and development, because it provides highly sensitive, quantitative and non-invasive measurements. PET imaging has the unequaled advantages over other biodistribution techniques to produce a complete pharmacokinetics time course study and to allow the direct comparison of different formulations in the same animal, thereby escaping the drawbacks of inter-individual variations and the need for large populations. PET offers particularly high return for the evaluation of the expensive new molecular drugs, which are often relatively large molecules experiencing major bioavailability issues. With respect to oligonucleotides, we have shown in a previous study that whole body distribution in monkeys could be assessed by PET imaging following IV injection (8). Although the Fluorine-18 labeling method used here has no significant effect on the biodistribution of a radiolabeled oligonucleotide, PET images depict the biodistribution of total radioactivity and do not take into account the metabolism of the radiotracer. For this reason, the present PET studies of different formulations of Dis-2 were conjugated with metabolite analysis performed on plasma from blood samples collected during the PET image acquisition with a sensitive competitive hybridization assay.

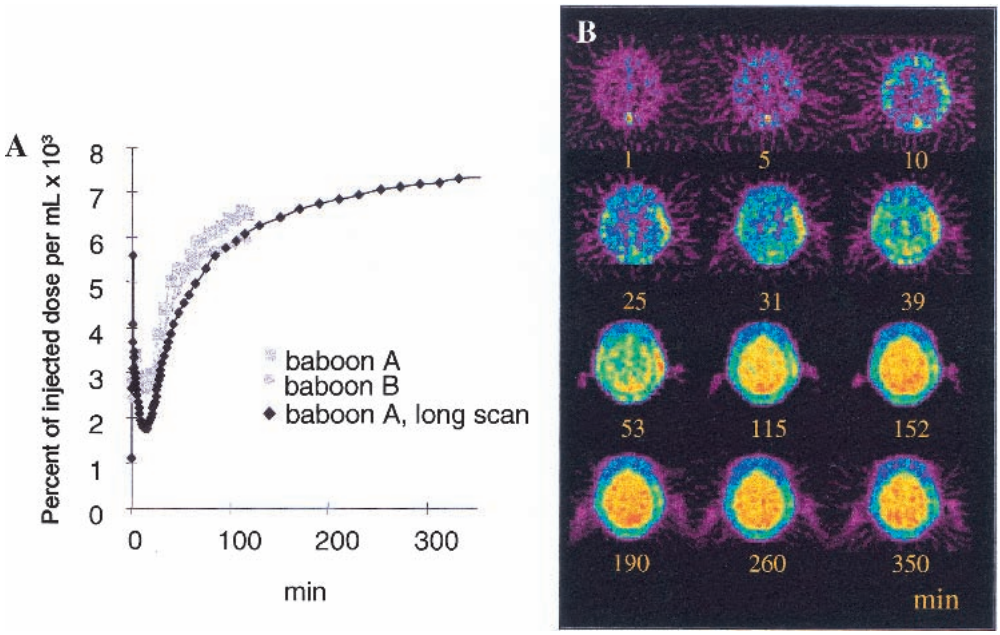

Fig. 5. Pharmacokinetics of NX1-vectorized Dis-2 in the brain area. **A**: Kinetics of radioactivity concentration (% of the injected dose per cc) in the brain; **B**: transaxial tomographic slices (2.425 mm thickness) corrected for radioactivity decay, acquired at the indicated time points after IV injection. Color scale from black (zero) to red (maximal uptake in the complete frame set for this brain slice).

In Vivo Protection from Plasmatic Nucleases

The increase of Dis-2 plasma stability resulting from the use of the vectors was detected by combining radio HPLC analysis with the competitive hybridization assay. This increase was modest when Dis-2 was associated with DD, but delivery with NX1 induced a major improvement of Dis-2 stability in plasma, with a 4-fold increase in $T_{1/2}$ β over the free oligonucleotide. Furthermore, there was a 7-fold increase in the distribution volume without modification of clearance, reflecting the extra protection against nucleases and a better extravasation (transport from blood to tissue) conferred to Dis-2 by NX1.

Plasma half lives of free phosphodiester and modified oligonucleotides reported in the literature range from 15 minutes or less to 50 h depending on the sequence, the length, the dose and the type of modification (15, 26–29). Tari *et al.* (30) found a $T_{1/2}$ β within 4 h for P-ethoxy modified oligonucleotide delivered with liposomes at a dose of 10 mg per kg of body weight in mice. However, these studies measured the total pool of radioactive species, uncorrected for metabolites, likely leading to an overestimation of the intact oligonucleotide's half-life in plasma. In the present study, intact Dis-2 was quantified separately through the combination of radio-HPLC and of a competitive hybridization assay, yielding a $T_{1/2}$ β of about 45 min for NX1/Dis-2 and about 10 min for free DIS-2. Direct comparison of the pharmacokinetics of a phosphodiester oligonucleotide administered in its free form and with a synthetic vector in the same animal brings strong support to the increase in plasmatic stability conferred by NX1.

Several hypotheses on the mechanism by which NX1 confers a better *in vivo* stability to oligonucleotides can be advanced, including its global negative charge, the atypical ultrastructure of the Neutraplex™ particles, a particular effect of one of the three lipids present in NX1 or the combination of any of these factors. One major reason for designing anionic or neutral vectors is to limit the non specific interaction with the negatively charged proteins present in the serum, which could induce a destabilization of the nucleic acid - vector complex as already reported in the case of cationic vectors (21). Accordingly, the effect induced by DD delivery on Dis-2 stability is slight as compared when using non-vectorized oligonucleotide. A negatively charged vector such as NX1 could combine the advantages of cationic vectors, i.e., the stabilization of the association between DNA and cationic lipids, and limit non-specific interactions *in vivo* by presenting a global negative charge to the medium.

Changes in Biodistribution Due to the Vectors

Major differences in radioactivity distribution were observed between the different formulations, except in the heart in which the pharmacokinetics where superimposable for all conditions, likely reflecting the absence of differences in the blood total radioactivity pharmacokinetics. Free Dis-2 showed a distribution typical of phosphodiester oligonucleotides as previously reported (8,15). Uptake of radioactivity was essentially observed in the two major elimination organs, liver and kidneys. In the liver, there was a biphasic time course typical of hepatic uptake and metabolism, while the kidneys showed the highest uptake with rapid elimination through the urinary tract. Other organs (heart, lungs, brain, muscle and spleen) showed negligible retention after the initial blood flow peak.

DD delivery led to an increase of uptake level of radioactivity in the liver and spleen. This distribution is typical of compounds taken up by the reticulo-endothelial system, and probably related to an opsonization mechanism known to be frequent with cationic complexes. Use of competitors of re-

ticulo-endothelial system targeting might help in evaluating this pharmacological observation. In the other organs tested, there were no differences between radioactivity uptake when using free Dis-2 or DD, suggesting that the small increase of stability induced by DD is insufficient to enhance uptake.

In contrast, dramatic changes in pharmacokinetics were observed with NX1, and these changes varied according to the organ examined. If not for the brain and lungs, the alteration of Dis-2 biodistribution with NX1 could, at least partially, have been explained by the potential of particles to distribute in the reticulo endothelial system. However, the lungs showed a much higher initial uptake with NX1 and a slower elimination after peak, leading to a 3- to 4-fold increase in the AUC_{120}. Pharmacokinetic analyses of lipid-based delivery systems have revealed that, in the case of systemic administration, movement from the circulation to organs is largely a unidirectional process and governed in large part by the size of the complexes. Thus, "first-pass" organs and those with a high blood flow (heart, lung, liver, spleen) exhibit significant uptake after intravenous administration due to the relatively large size of the lipid-nucleic acid complexes.

However, the most impressive change with NX1 was observed in the brain, which depicted pharmacokinetics and biodistribution not previously described. While the initial peak of radioactivity uptake was not different for NX1 compared to free Dis-2, a second phase of uptake started at 30 min after IV injection, and was maintained continuously over 6 h. This phase corresponded with a dramatic modification of the radioactivity distribution observed on PET images of the cephalic area, which shifted from peri-cerebral structures to the cerebral area. At the resolution level of PET images, it is not possible to gain a deeper insight into this observation, and further experiments are needed in smaller laboratory species in which invasive procedures are easier to perform, using isotopes with better intrinsic resolution than fluorine-18. One possibility is that the cerebral uptake of radioactivity observed with NX1 is due to a metabolite of Dis-2, although it is unlikely that NX1 vectorization would lead to a different pathway of metabolism for the oligonucleotide. Alternatively, *in vivo* reassociation of the vector with a labeled metabolite to form a new complex with special affinity for brain tissue appears highly improbable, and in any case would not contradict the fact that NX1 does increase cerebral uptake of radioactivity. Moreover, results suggest that NX1 delivery has a protective effect, since intact Dis-2 was detected for at least 2 h after IV injection. Due to its specific ultrastructure, NX1/Dis-2 complexes might lead to a slow but steady uptake of radioactivity by the cerebral tissue, even though it should be noted that the amount of radioactivity taken up by brain tissue remains very small ($<10^{-4}$ of injected dose). It remains also to be determined whether this special affinity of brain tissue for NX1 complex is restricted to the brain microvasculature or implies the cerebral parenchyma. In this respect, it is noteworthy that the images do not show significant regional distribution in specific cerebral structures detectable with our PET system.

In summary, we have shown that (a) PET imaging yields *in vivo* quantitative pharmacokinetics information that is ideal to evaluate the modifications induced by vectors in the biodistribution and organ bioavailability of the oligonucleotide; (b) competitive hybridization pictures the capacity of synthetic vectors to enhance *in vivo* stability; and (c) the combination of these two techniques is able to demonstrate that carefully tailored anionic vectors of the Neutraplex™ type dramatically ameliorate the *in vivo* delivery of an oligonucleotide.

ACKNOWLEDGMENTS

We thank Dr Marc Joliot (Cyceron, Caen) for the image normalization software and Antoinette Jobert (INSERM U 334) for help with the animal experiments. Supported in part by Biomed2 contract N° BMH4-CT96-1067, MESR ACC-SV12 contract N° 2654, and the Association Française contre les Myopathies.

REFERENCES

1. C. A. Stein. Phosphorothioate antisense oligodeoxynucleotides: questions of specificity. *Trends Biotechnol.* **14**:147–149 (1996).
2. A. Prochiantz. Peptide nucleic acid smugglers. *Nat. Biotechnol.* **16**:819–820 (1998).
3. P. L. Felgner, Y. Barenholz, J. P. Behr, S. H. Cheng, P. Cullis, L. Huang, J. A. Jessee, L. Seymour, F. Szoka, A. R. Thierry, E. Wagner, and G. Wu. Nomenclature for synthetic gene delivery systems. *Hum. Gene Ther.* **8**:511–512 (1997).
4. A. R. Thierry, P. Rabinovich, B. Peng, L. C. Mahan, J. L. Bryant, and R. C. Gallo. Characterization of liposome-mediated gene delivery: expression, stability and pharmacokinetics of plasmid DNA. *Gene Ther.* **4**:226–237 (1997).
5. R. J. Lee and L. Huang. Lipidic vector systems for gene transfer. *Crit. Rev. Ther. Drug Carrier Syst.* **14**:173–206 (1997).
6. T. Jones. The imaging science of positron emission tomography. *Eur. J. Nucl. Med.* **23**:807–813 (1996).
7. T. Jones. The role of positron emission tomography within the spectrum of medical imaging. *Eur. J. Nucl. Med.* **23**:207–211 (1996).
8. B. Tavitian, S. Terrazzino, B. Kuhnast, S. Marzabal, O. Stettler, F. Dollé, J. R. Deverre, A. Jobert, F. Hinnen, B. Bendriem, C. Crouzel, and L. Di Giamberardino. In vivo imaging of oligonucleotides with positron emission tomography. *Nat. Med.* **4**:467–471 (1998).
9. J. R. Deverre, V. Boutet, D. Boquet, E. Ezan, J. Grassi, and J. M. Grognet. A competitive enzyme hybridization assay for plasma determination of phosphodiester and phosphorothioate antisense oligonucleotides. *Nucleic Acids Res.* **25**:3584–3589 (1997).
10. C. Lavigne, J. Yelle, G. Sauvé, and A.R. Thierry. Lipid-based delivery of combinations of antisense oligodeoxynucleotides for the in vitro inhibition of HIV-1 replication. *AAPS Pharm. Sci.* **3**:7 (2001).
11. F. Dollé, F. Hinnen, F. Vaufrey, B. Tavitian, and C. Crouzel. A general method for labeling oligodeoxynucleotides with 18F for in vivo PET imaging. *J. Label Compounds Radiopharm.* **39**:319–330 (1997).
12. C. Lavigne and A. R. Thierry. Enhanced antisense inhibition of human immunodeficiency virus type 1 in cell cultures by DLS delivery system. *Biochem. Biophys. Res. Commun.* **237**:566–571 (1997).
13. M. Schmutz, D. Durand, A. Debin, Y. Palvadeau, A. Etienne, and A.R.Thierry. DNA packing in stable lipid complexes designed for gene transfer imitates DNA compaction in bacteriophage. *Proc. Natl. Acad. Sci. USA* **96**:12293–12298 (1999).
14. MP. Audrezet, G. Le Bolch, V. Floch, JJ. Yaounac, JC. Clement, H. des Abbayes, B. Mercier, A. Paul, and C. Ferec. Novel cationic phospholipids agents for gene transfer to a Cystic fibrosis cell line. *J. Liposome Res.* **7**:273–300 (1997).
15. S. Agrawal, J. Temsamani, W. Galbraith, and J. Tang. Pharmacokinetics of antisense oligonucleotides. *Clin. Pharmacokinet.* **28**: 7–16 (1995).
16. C. Plank, K. Mechtler, F. C. Szoka, Jr., and E. Wagner. Activation of the complement system by synthetic DNA complexes: a potential barrier for intravenous gene delivery. *Hum. Gene Ther.* **7**:1437–1446 (1996).

17. A. R. Thierry. Optimization of lipoplex formulations for intravenous gene delivery. *J. Liposome Res.* **7**:143–159 (1997).
18. A. R. Thierry and A. Dritschilo. Intracellular availability of unmodified, phosphorothioated and liposomally encapsulated oligodeoxynucleotides for antisense activity. *Nucleic Acids Res.* **20**: 5691–5698 (1992).
19. R. L. Juliano and S. Akhtar. Liposomes as a drug delivery system for antisense oligonucleotides. *Antisense Res. Dev.* **2**:165–176 (1992).
20. C. Ropert, Z. Mishal, Jr., J. M. Rodrigues, C. Malvy, and P. Couvreur. Retrovirus budding may constitute a port of entry for drug carriers. *Biochim. Biophys. Acta* **1310**:53–59 (1996).
21. D. C. Litzinger. Limitations of cationic liposomes for antisense oligonucleotide delivery in vivo. *J. Liposome Res.* **7**:51–61 (1997).
22. J. P. Yang and L. Huang. Overcoming the inhibitory effect of serum on lipofection by increasing the charge ratio of cationic liposome to DNA. *Gene Ther.* **4**:950–960 (1997).
23. A. R. Thierry and L. C. Mahan. Therapeutic Applications of lipid-based Gene Delivery systems. In A. Rolland (ed.), *Advanced Gene Delivery*, Harwood Academic, Amsterdam, pp 124–137 (1998).
24. A. R. Thierry, Y. Lunardi-Iskandar, J. L. Bryant, P. Rabinovich, R. C. Gallo, and L. C. Mahan. Systemic gene therapy: biodistribution and long-term expression of a transgene in mice. *Proc. Natl. Acad. Sci. USA* **92**:9742–9746 (1995).
25. O. A. Sedelnikova, I. G. Panyutin, A. R. Thierry, and R. D. Neumann. Radiotoxicity of iodine-125-labeled oligodeoxyribonucleotides in mammalian cells. *J. Nucl. Med.* **39**:1412–1418 (1998).
26. R. Zhang, R. B. Diasio, Z. Lu, T. Liu, Z. Jiang, W. M. Galbraith, and S. Agrawal. Pharmacokinetics and tissue distribution in rats of an oligodeoxynucleotide phosphorothioate (GEM 91) developed as a therapeutic agent for human immunodeficiency virus type-1. *Biochem. Pharmacol.* **49**:929–939 (1995).
27. P. L. Iversen, J. Mata, and W. G. Tracewell. and G. Zon. Pharmacokinetics of an antisense phosphorothioate oligodeoxynucleotide against rev from human immunodeficiency virus type 1 in the adult male rat following single injections and continuous infusion. *Antisense Res. Dev.* **4**:43–52 (1994).
28. F. I. Raynaud, R. M. Orr, P. M. Goddard, H. A. Lacey, H. Lancashire, I. R. Judson, T. Beck, B. Bryan, and F. E. Cotter. Pharmacokinetics of G3139, a phosphorothioate oligodeoxynucleotide antisense to bcl-2, after intravenous administration or continuous subcutaneous infusion to mice. *J. Pharmacol. Exp. Ther.* **281**:420–427 (1997).
29. R. K. DeLong, A. Nolting, M. Fisher, Q. Chen, E. Wickstrom, M. Kligshteyn, S. Demirdji, M. Caruthers, and R. L. Juliano. Comparative pharmacokinetics, tissue distribution, and tumor accumulation of phosphorothioate, phosphorodithioate, and methylphosphonate oligonucleotides in nude mice. *Antisense Nucleic Acid Drug Dev.* **7**:71–77 (1997).
30. A. Tari, N. Neamati, M. Andreff, and G. Lopez-Berenstein. Liposomal delivery of P-ethoxy antisense oligonucleotides in chronic myelogenous leukemia. In G. Gregoriadis (ed.), *Targeting of drugs: Strategies for oligonucleotide and gene delivery in therapy*, Plenum Press, New York, 1996 pp. 163–168.